# Hippocampal Subregions Are Differentially Affected in the Progression to Alzheimer's Disease

**SARAH J. GREENE[1,2] AND RONALD J. KILLIANY[2,3,4*]; THE ALZHEIMER'S DISEASE NEUROIMAGING INITIATIVE**

[1]Department of Anatomy and Neurobiology, University of Vermont College of Medicine, Burlington, Vermont 05405-0068

[2]Department of Anatomy and Neurobiology, Boston University School of Medicine, Boston, Massachusetts 02118

[3]Center for Biomedical Imaging, Boston University School of Medicine, Boston, Massachusetts 02118

[4]Department of Environmental Health, Boston University School of Public Health, Boston, Massachusetts 02118

ABSTRACT

Atrophy within the hippocampus (HP) as measured by magnetic resonance imaging (MRI) is a promising biomarker for the progression to Alzheimer's disease (AD). Subregions of the HP along the longitudinal axis have been found to demonstrate unique function, as well as undergo differential changes in the progression to AD. Little is known of relationships between such HP subregions and other potential biomarkers, such as neuropsychological (NP), genetic, and cerebral spinal fluid (CSF) beta amyloid and tau measures. The purpose of this study was to subdivide the hippocampus to determine how the head, body, and tail were affected in normal control, mild cognitively impaired, and AD subjects, and investigate relationships with HP subregions and other potential biomarkers. MRI scans of 120 participants of the Alzheimer's Disease Neuroimaging Initiative were processed using FreeSurfer, and the HP was subdivided using 3D Slicer. Each subregion was compared among groups, and correlations were used to determine relationships with NP, genetic, and CSF measures. Results suggest that HP subregions are undergoing differential atrophy in AD, and demonstrate unique relationships with NP and CSF data. Discriminant function analyses revealed that these regions, when combined with NP and CSF measures, were able to classify by diagnostic group, and classify MCI subjects who would and would not progress to AD within 12 months. Anat Rec, 295:132–140, 2012. © 2011 Wiley Periodicals, Inc.

Grant sponsor: National Institutes of Health Grant; Grant numbers: U01 AG024904, AG000277, P30 AG010129, K01 AG030514; Grant sponsors: The National Institute on Aging, The National Institute of Biomedical Imaging and Bioengineering, Abbott, AstraZeneca AB, Bayer Schering Pharma AG, Bristol-Myers Squibb, Eisai Global Clinical Development, Elan Corporation, Genentech, GE Healthcare, GlaxoSmithKline, Innogenetics, Johnson and Johnson, Eli Lilly and Co., Medpace, Inc., Merck and Co., Inc, Novartis AG, Pfizer Inc, F. Hoffman-La Roche, Schering-Plough, Synarc, Inc., and Wyeth, The Alzheimer's Association and Alzheimer's Drug Discovery Foundation; Grant sponsor: The U.S. Food and Drug Administration, Dana Foundation.

Data used in the preparation of this article were obtained from the Alzheimer's Disease Neuroimaging Initiative (ADNI) database (www.loni.ucla.edu\ADNI). As such, the investigators within the ADNI contributed to the design and implementation of ADNI and/or provided data but did not participate in analysis or writing of this report. ADNI investigators include (complete listing available at www.loni.ucla.edu\ADNI\Collaboration\ADNI_Authorship_list.pdf).

*Correspondence to: Ronald J. Killiany, Department of Anatomy and Neurobiology, Boston University School of Medicine, 700 Albany Street, W701, Boston, MA 02118. Fax: 617-638-4922. E-mail: killiany@bu.edu

Received 1 June 2011; Accepted 4 September 2011

DOI 10.1002/ar.21493

Published online 18 November 2011 in Wiley Online Library (wileyonlinelibrary.com).

**Key words: Alzheimer's disease; MCI; MRI; neuropsychology; FreeSurfer**

## INTRODUCTION

Atrophy within the hippocampus in the progression to Alzheimer's disease (AD) has been well established. The hippocampus is one of the earliest regions in the brain for neurofibrillary tangle (NT) development in AD (Braak and Braak, 1991; Braak et al., 1993), and such pathology has also been found in non-demented individuals at the time of death, (Ulrich, 1985; Price et al., 1991; Bouras et al., 1993, 1994; Giannakopoulos et al., 1994; Haroutunian et al., 1999; Price and Morris, 1999) suggesting that they were in the process of developing Alzheimer's disease. Several imaging studies have identified the hippocampus as an MRI measure useful in identifying prodromal AD (Fox et al., 1996; Convit et al., 2000; Callen et al., 2001; Csernansky et al., 2005). Increased rates of atrophy of medial temporal regions have been associated with decline to AD (Killiany et al., 2002; Buckner et al., 2005; Chetelat et al., 2005; Desikan et al., 2008). Baseline hippocampal measures have also been demonstrated to predict future conversion to AD (Jack et al., 2005; den Heijer et al., 2006; Devanand et al., 2007, 2008; Fleisher et al., 2008; Risacher et al., 2009).

The hippocampus is histologically subdivided transversely into several subfields, including the dentate gyrus, subiculum, and cornu ammonis subfields (CA1-CA4), which have unique connections to other subcortical and cortical regions in the brain. Imaging studies have used methods for identifying these hippocampal subfields through unfolding methods in high resolution functional MRI (Zeineh et al., 2000, 2001; Ekstrom et al., 2009) and high resolution *in vivo* (Mueller et al., 2007; Theysohn et al., 2009; Van Leemput et al., 2009) and *ex vivo* (Yushkevich et al., 2009) structural MRI mapping. These subfields are independent of subregional definitions of the hippocampus along its longitudinal axis (head, body, and tail) that are more readily evaluated in lower resolution imaging studies. Malykhin et al. (2010) recently investigated relationships between hippocampal subfields and subregions in 4.7 tesla scans, and reported that while all subfields were present within the head, body, and tail of the hippocampus, a majority of the dentate gyrus was within the hippocampal body, while a majority of C1–C3 were in the hippocampal head.

Although unique functional roles along the anterior–posterior axis of the hippocampus have been reported in fMRI and PET studies (Lepage et al., 1998; Strange et al., 1999; Chua et al., 2007; Rosazza et al., 2009), few studies have addressed the differential effects of AD on the head, body, and tail of the hippocampus as measured by structural MRI. There is evidence that the hippocampal head and body undergo increased atrophy in mild cognitive impairment (MCI) (Martin et al., 2010), and these subregions are correlated with neuropsychological measures of memory (Hackert et al., 2002; Chen et al., 2010). Differential atrophy within the head, body, and tail of the hippocampus have additionally been reported in other disease states, such as hippocampal sclerosis (Bronen et al., 1995), Parkinson's disease (Bouchard et al., 2008), temporal lobe epilepsy (Bernasconi et al., 2003), and schizophrenia (Witthaus et al., 2010), further suggesting that these hippocampal subregions may be sensitive to detecting progression to different disease states, including AD.

An inverse relationship has been found between cerebral spinal fluid (CSF) beta amyloid ($A\beta_{42}$) and Aß deposition in the brain (Strozyk et al., 2003; Tapiola et al., 2009), and CSF tau has been shown to reflect NT pathology in the brain (Blennow et al., 1995; Tapiola et al., 1997), therefore, suggesting these measures may be effective in identifying AD neuropathology occurring within the brain. Although Aß pathology remains sparse in the hippocampus, associations between hippocampal atrophy and beta amyloid deposition as measured by Pittsburgh Compound B (PIB) retention have been reported (Jack et al., 2008b; Mormino et al., 2009; Storandt et al., 2009; Bourgeat et al., 2010; Chetelat et al., 2010). Recent studies have, therefore, investigated the role of combining CSF biomarkers of $A\beta_{42}$ and tau with MRI imaging measures in identifying individuals in preclinical stages of AD (de Leon et al., 2007; Walhovd et al., 2010). Little is known of the relationship between such CSF measures and volumes of hippocampal head, body, and tail subregions in AD, or how these measures in combination with one another and with neuropsychological data may serve as biomarkers for the progression to AD.

In this study, the hippocampus was subdivided into three regions along its long axis: the head, body, and tail, to determine if these subregions are differentially affected in the progression to AD, and if these subregions are associated with neuropsychological performance and CSF measures of $A\beta_{42}$, total tau, and phosphorylated tau in normal (NC), MCI, and AD participants of the Alzheimer's Disease Neuroimaging Initiative (ADNI).

## MATERIALS AND METHODS

### Study Population

Data used in the preparation of this article were obtained from the Alzheimer's Disease Neuroimaging Initiative (ADNI) database (www.loni.ucla.edu\ADNI). The ADNI was launched in 2003 by the National Institute on Aging (NIA), the National Institute of Biomedical Imaging and Bioengineering (NIBIB), the Food and Drug Administration (FDA), private pharmaceutical companies and non-profit organizations, as a $60 million, 5-year public–private partnership. The primary goal of ADNI has been to test whether serial magnetic resonance imaging (MRI), positron emission tomography (PET), other biological markers, and clinical and neuropsychological assessment can be combined to measure

the progression of MCI and early AD. Determination of sensitive and specific markers of very early AD progression is intended to aid researchers and clinicians to develop new treatments and monitor their effectiveness, as well as lessen the time and cost of clinical trials.

The principle investigator of this initiative is Michael W. Weiner, M.D., VA Medical Center and University of California, San Francisco. ADNI is the result of efforts of many co-investigators from a broad range of academic institutions and private corporations, and subjects have been recruited from over 50 sites across the United States and Canada. The initial goal of ADNI was to recruit 800 adults, ages 55 to 90, to participate in the research—~200 cognitively normal older individuals to be followed for 3 years, 400 people with MCI to be followed for 3 years, and 200 people with early AD to be followed for 2 years.

For this study, 120 subjects from the ADNI (40 NC, 40 MCI, 40 AD; Table 1) were randomly selected from each group while being matched for gender. Subjects were administered a neuropsychological (NP) battery at screening, and MRI and CSF measures were obtained at baseline. Conversion at follow-up data was available for a subset of MCI individuals.

## MRI Acquisition and Postprocessing

The raw dicom data from two T1-weighted sagittal 3D MP-RAGE MRI acquisitions for each of the 120 participants included in this study was downloaded from the ADNI database (www.loni.ucla.edu\ADNI). The protocol for scan acquisition and calibration for the ADNI has been described elsewhere (Jack et al., 2008a).

Hippocampal measures from all scans were obtained from FreeSurfer, version 4.3.1 (http://surfer.nmr.mgh.harvard.edu/). The methodology of FreeSurfer has been described in detail (Dale and Sereno, 1993; Dale et al., 1999; Fischl et al., 1999; Fischl and Dale, 2000; Fischl et al., 2001, 2002, 2004a,b; Segonne et al., 2004; Desikan et al., 2006; Han et al., 2006; Jovicich et al., 2006; Segonne et al., 2007). Hippocampal measures were based on subcortical segmentation (Fischl et al., 2002, 2004a; Buckner et al., 2004), and a neuroanatomically trained operator reviewed images for accuracy.

Once scans were processed through FreeSurfer, output was loaded into 3D Slicer (http://www.slicer.org/). The FreeSurfer boundaries of the hippocampus were maintained and subdivided into the head, body, and tail. These subregions were manually defined in a manner similar to that described by Martin et al. (2010) (Fig. 1). The head–body boundary was identified in the sagittal plane, and the body–tail boundary was defined in the coronal plane as the first slice where the fimbria of the fornix was evident. Operators were blind to diagnostic status and gender of all participants included in this study. A subset of scans ($n = 5$) was re-evaluated to determine intrarater and inter-rater reliability, and the mean correlation between tracings was 0.98 and 0.99, respectively.

**TABLE 1. Demographics for 120 ADNI participants**

| | Normal | MCI | AD |
|---|---|---|---|
| Gender | 50% F | 50% F | 50% F |
| Age | 76.57 | 74.47 | 76.34 |
| Education | 16.15 | 15.58 | 14.78 |
| MMSE | 28.93 | 26.83 | 23.28 |

## Neuropsychological Testing

All participants underwent NP testing at the baseline visit. This battery included the Alzheimer's Disease Assessment Scale Cognitive exam (Rosen et al., 1984), Clock Drawing Test, Auditory Verbal Learning test (AVLT) (Rey, 1964), Digit Span Forward and Backward, Category Fluency, Trail making A and B (Reitan, 1958), Wechsler Adult Intelligence Scale-Revised (WAIS-R) Symbol Digit Substitution, Boston Naming Test (Kaplan et al., 1983), AVLT 30 min Delay, and the American National Adult Reading Test. In addition, participants were given the Mini Mental Status Exam (MMSE) (Folstein et al., 1975) at each visit.

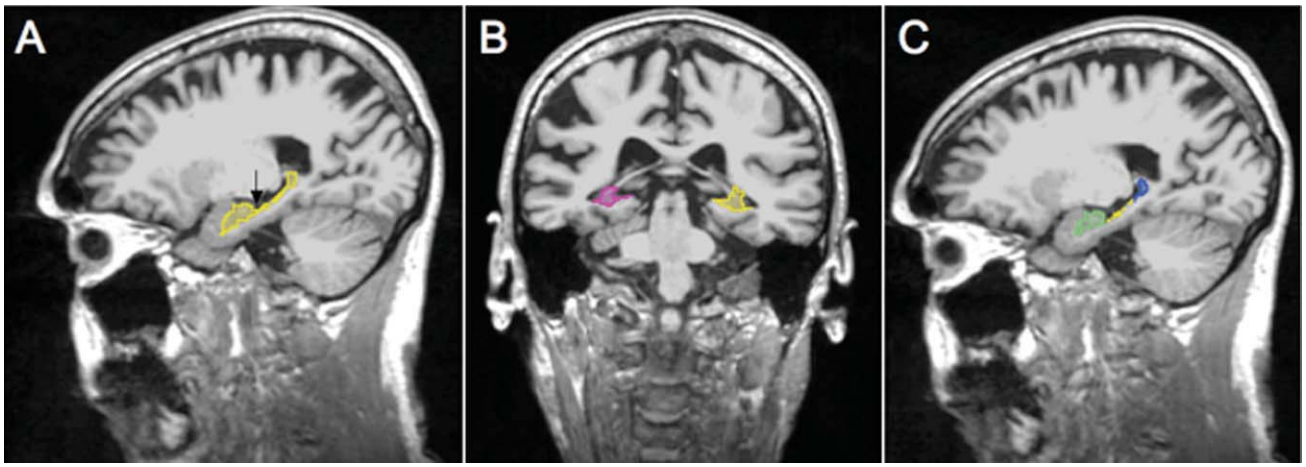


Fig. 1. Methods for identifying boundaries for the head, body, and tail of the hippocampus. **A**: Arrow is pointing to the head/body boundary. **B**: View of body/tail boundary in left hemisphere where the fimbria of the fornix comes into view; body/tail boundary. **C**: Subregions after relabeling has been completed (green: head; yellow: body; blue: tail).

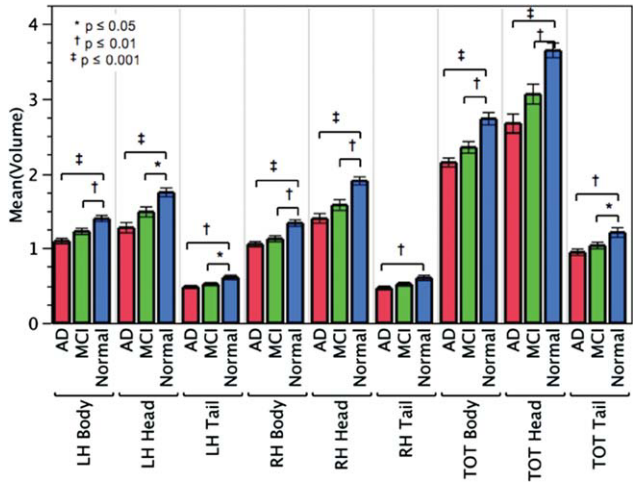


Fig. 2. Group differences in left, right, and combined left/right hippocampal head, body, and tail measures.

### CSF Measures

Measures of CSF Aß$_{42}$, total tau (t-tau), and tau phosphorylated at the threonine 181 (p-tau) taken at the baseline visit were available for a subset of participants included in this study ($n$ = 59). The specific CSF markers included in the ADNI study were selected based on their high priority as potential biomarkers, as determined by AD biomarker experts (Frank et al., 2003; Reckess, 2003) and consultants for the study (http://www.adni-info.org).

Methods for CSF collection have been described in detail elsewhere (www.adni-info.org; Shaw et al., 2009). CSF was collected in the morning after an overnight fast. The lumbar puncture was performed in the lateral decubitus or sitting position, depending on each participant's preference. After the site was prepared and numbed with Lidocaine, a 24-guage atraumatic spinal needle and introducer was used, and CSF was collected into polypropylene vials after the first 1–2 mL were discarded to clear the sample of blood. Two microliters of CSF were used for cell counting and for protein and glucose measures. The remainder of the sample was transferred into polypropylene transfer tubes, frozen within one hour, and packed in dry ice. Samples were sent overnight to the University of Pennsylvania Medical Center AD Biomarker Fluid Bank Laboratory. Samples were then thawed, aliquoted, and stored in −80°C freezers. Measures of Aß$_{42,}$ t-tau, and p-tau were taken using the Innogenetics immunoassay kit (INNO- AlzBio3 Ghent, Belgium; reagents are for research-use only) with Luminex platform (Luminex Corp, Austin, TX), using monoclonal antibodies 4D7A3, AT120, and AT270 for Aß$_{42}$, t-tau, and p-tau, respectively. Assays were performed in duplicate and averaged.

### Statistical Analyses

Kruskal-Wallis tests were run to determine if groups differed significantly in age or education. Multivariate analyses of variance (MANOVA) were used to determine group differences in left, right, and total hippocampal subregions. Pearson correlations were completed to determine relationships between MRI, NP, Apolipoprotein E epsilon 4 (APOE-ε4) load, and CSF measures. Discriminant function analyses were run to determine the most effective combination of MRI, NP, and CSF measures for classifying groups and predicting future conversion to AD in MCI individuals.

## RESULTS

Groups did not significantly differ in age or education (Table 1). Pearson correlations revealed no significant correlation between intracranial volume (ICV) and hippocampal measures, analysis of variance (ANOVA) revealed no difference in ICV between groups, and Chi Square analysis revealed no ICV gender difference across all groups in this population. Therefore, raw hippocampal measures (uncorrected for ICV) were included in analyses. The results of MANOVA comparing right and left head, body, and tail, as well as combined left/right hippocampal volumes are outlined in Figure 2. Pearson correlations revealed significant associations between the right entorhinal cortex and the right hippocampal head (r = 0.614; $P < 0.001$), body (r = 0.547, $P < 0.001$), and tail (r = 0.317, $P < 0.01$), and between the left entorhinal cortex and the left hippocampal head (r = 0.628, $P < 0.001$), body (r = 0.494, $P < 0.001$), and tail (r = 0.366; $P < 0.001$).

A principle components analysis was completed to identify NP tests to include in correlations with hippocampal and CSF data. This revealed five factors, and one test was selected from within each factor for correlations: Auditory Verbal Learning 30 min Delay (AV-Delay), Boston Naming Test, Digit Symbol, Digit Span Backwards, and Clock Command. Pearson correlations revealed that Clock Command correlated with the right head (r = 0.316; $P < 0.01$), combined right/left head (r = 0.265; $P < 0.01$), and left body (r = 0.264; $P < 0.01$; the Boston Naming Test correlated with the right head (r = 0.356; $P < 0.001$), left head (r = 0.444; $P < 0.001$), combined right/left head (r = 0.424; $P < 0.001$), left body (r = 0.329; $P < 0.001$), combined right/left body (r = 0.281; $P < 0.01$), right tail (r = 0.215; $P < 0.05$), left tail (r = 0.303; $P < 0.01$), and combined right/left tail (r = 0.269; $P < 0.01$); and AV Delay correlated with the right head (r = 0.428; $P < 0.001$), left head (r = 0.438; $P < 0.001$), combined right/left head (r = 0.460; $P < 0.001$), right body (r = 0.350; $P < 0.001$), left body (r = 0.343; $P < 0.001$), combined right/left body (r = 0.374; $P < 0.001$), left tail (r = 0.243, $P < 0.05$), and combined right/left tail (r = 0.211, $P < 0.05$). APOE-ε4 load did not correlate with any hippocampal or NP measures.

The left, right, and combined left/right hippocampal head, body, and tail volumes were entered into a discriminant function analyses to determine which measures were best able to correctly classify group membership ($n$ = 120). This was demonstrated to be the combined left/right head and body, which were able to classify NC, MCI, and AD with 67.5%, 17.5%, and 65% accuracy, respectively. When entorhinal volume was included, the combined left/right entorhinal volume was able to predict these groups with 70%, 32.5%, 70% accuracy. NP measures were then entered with hippocampal measures (three AD subjects were excluded due to incomplete NP data), which resulted in a combination of AV Immediate and Delay, Digit Symbol and the left

hippocampal body being able to classify NC, MCI, and AD with 85%, 80%, and 74.4% accuracy, respectively. Entering APOE-ε4 load did not improve classification.

Analyses were completed in the 59 subjects where CSF measures were available (22 NC, 17 MCI, 20 AD; Table 2). MANOVA assessing CSF measures indicated that the only difference between NC and MCI was in $A\beta_{42}$ ($P < 0.001$), while total tau, p-tau, and $A\beta_{42}$ were significantly different between NC and AD ($P < 0.01$). Pearson correlations between CSF and hippocampal measures (Table 3) revealed that the combined left/right hippocampal head was the only hippocampal measure associated with t-tau ($r = -0.261$, $P < 0.05$). $A\beta_{42}$ correlated with the left head ($r = 0.329$, $P < 0.05$), combined left/right head ($r = 0.288$, $P < 0.05$), left body ($r = 0.289$; $P < 0.05$), combined left/right body ($r = 0.284$, $P < 0.05$), right tail ($r = 0.326$, $P < 0.05$), left tail ($r = 0.418$, $P < 0.001$), and combined left/right tail ($r = 0.402$, $P < 0.01$). There were no significant correlations between hippocampal measures and p-tau. The only measure that was found to correlate with APOE-ε4 status was CSF $A\beta_{42}$ ($r = -0.560$, $P < 0.001$).

Fifty-eight participants (22 NC, 17 MCI, 19 AD) had complete MRI, NP, and CSF measures available (one AD subject had incomplete NP data). The same NP measures were included as those in the entire group as described above to determine relationships between CSF and cognition. Correlations between CSF and NP measures are presented in Table 3. Discriminant function analyses were run to determine the most accurate predictors of group membership. When hippocampal measures were entered alone in this subgroup, the combined left/right hippocampal head was able to classify NC, MCI, and AD with 72.7%, 35.3%, and 69% accuracy, respectively. When hippocampal measures were combined with CSF measures, a combination of CSF $A\beta_{42}$ and combined left/right hippocampal head volume was able to classify NC, MCI, and AD with 81.8%, 52.9%, and 60% accuracy. Entorhinal measures were then included, which resulted in the left entorhinal and $A\beta_{42}$ predicting group membership with 72.7%, 52.9%, 60% accuracy. When NP, hippocampal, entorhinal, CSF, and APOE-ε4 measures were entered, it was found that a combination of AV Immediate and Delay, Digit Symbol, left hippocampal body, and right hippocampal tail were able to classify NC, MCI, and AD with 95.5%, 82.4%, and 78.9% accuracy, respectively.

At the 12-month follow-up visit, 11 MCI subjects had converted to AD. These subjects were matched for age and education with MCI subjects who remained stable at the 12-month follow-up visit. Baseline measures of hippocampal volume, NP performance, CSF, and APOE-ε4 load were evaluated in both the stable and converter groups. Groups did not significantly differ in hippocampal or NP measures. Discriminant function analyses were run to determine predictors for future conversion to AD. No hippocampal or entorhinal measures predicted decline, however, a combination of Digit Symbol and Categories scores were able to predict stable versus converter subjects with 72.7% and 90.1% accuracy. CSF measures were available for six MCI subjects who later converted to AD. A second discriminant function analysis was run to determine if a combination of CSF, hippocampal, APOE-ε4 load, and NP measures were able to predict future conversion. In this small population of subjects, a combination of phosphorylated tau, total tau/beta amyloid ratio, Digit Symbol, Categories, Trails B, and combined left/right hippocampal head volume were able to predict stable versus converters with 100% accuracy.

**TABLE 2. Demographics for 59 subjects with CSF data**

| | Normal | MCI | AD |
|---|---|---|---|
| Gender | 36% F | 47% F | 45% F |
| Age | 76.77 | 75.89 | 74.57 |
| Education | 16 | 15.94 | 14.4 |
| MMSE | 28.72 | 26.59 | 23.6 |

## DISCUSSION

Few studies have investigated how subregions of the hippocampus are affected in the progression to AD, and even fewer have been able to combine these measures, with APOE-ε4 load, NP performance, and CSF measures to determine how these variables interact, and therefore may provide a profile of those who are at risk for

**TABLE 3. Correlations between CSF, NP, and hippocampal measures**

| | CSF $Abeta_{42}$ | CSF T-tau | CSF $P\text{-}tau_{181}$ |
|---|---|---|---|
| NP measures (r values) | | | |
| Clock command total | 0.1705 | −0.3407† | −0.2180 |
| Digit span backward total | 0.0477 | −0.1691 | −0.1456 |
| Digit symbol total correct | 0.3541† | −0.4689‡ | −0.6148‡ |
| BNT total correct | 0.2513 | −0.3358† | −0.3474† |
| AV 30 minute delay | 0.6006‡ | −0.3910† | −0.3677† |
| Hippocampal measures (r values) | | | |
| Right hippocampal head | 0.2088 | −0.2364 | −0.2236 |
| Left hippocampal head | 0.3290* | −0.2496 | −0.2465 |
| Right + Left hippocampal head | 0.2882* | −0.2612* | −0.2526 |
| Right hippocampal body | 0.2433 | −0.0251 | −0.0789 |
| Left Hippocampal body | 0.2891* | −0.1751 | −0.1271 |
| Left + Right hippocampal body | 0.2844* | −0.1090 | −0.1105 |
| Right hippocampal tail | 0.3258* | −0.0720 | −0.0965 |
| Left hippocampal tail | 0.4179‡ | −0.1495 | −0.0935 |
| Left + Right hippocampal tail | 0.4015† | −0.1170 | −0.1040 |

$P < 0.05$, †$P < 0.01$, ‡$P < 0.001$.

developing AD. The purpose of the current study was to determine if MRI measures of the head, body, and tail of the hippocampus were differentially affected in normal aging, MCI, and AD, and how these measures interacted with APOE-ε4, CSF, and NP measures to provide accurate classification by diagnostic group and predict future decline to AD.

The first objective of this study was to determine if the head, body, and tail of the hippocampus were differentially affected in normal aging, MCI, and AD. An overall analysis revealed that these subregions were different between diagnostic groups. Follow-up comparisons demonstrated differences between NC and MCI in the left, right and combined left/right head and body, with the largest difference in the combined left/right volume of the head of the hippocampus. Interestingly, no measures were significantly different between MCI and AD, suggesting that these changes are occurring very early in the progression to AD, and are most pronounced in the rostral hippocampal subregions such as the head and body. Studies have demonstrated changes in glucose metabolism (Ouchi et al., 1998) and diffusivity (Yushkevich et al., 2010) in the head of the hippocampus in subjects with AD, which may contribute to these early volumetric differences. Discriminant function analyses provided evidence that the combined left/right volumes of the head and body of the hippocampus were best able to accurately classify by diagnostic groups when hippocampal measures were entered alone. This supports the work of Martin et al. (2010) who reported primary atrophy of anterior hippocampal regions in normal subjects who later progressed to MCI. Interestingly, in the current study, there were no baseline regional hippocampal differences between stable MCI subjects and MCI subjects who converted to AD at one-year follow-up, suggesting that perhaps these changes are even occurring prior to an individual entering into the MCI phase of the disease.

The second objective in this study was to explore relationships between hippocampal subregions, NP, and CSF measures to determine the effectiveness of these variables in classifying by diagnostic groups, as well as predicting future conversion to AD. When performing correlations with NP measures, most relationships were found with the hippocampal head and body. The right, left, and combined left/right volumes of the hippocampal head and body measures correlated with delayed recall, though the strongest correlations were with hippocampal head. All but the right body and tail correlated with total correct score of the Boston Naming Test, again with the strongest correlations being with the volume of the hippocampal head. The right and combined left/right volume of the hippocampal head, as well as the left body and tail correlated with Clock Command scores. Other studies have yielded similar results, where relationships between volumes of the hippocampal head (Hackert et al., 2002) and body (Chen et al., 2010) and verbal memory have been reported in non-demented individuals. Although Chen et al. (2010) found this relationship only in the left hippocampal body, the current study found both the left and right head and body to be correlated with AV-Delay. These associations may be due to disruption of the perforant pathway, a connection between the entorhinal cortex and hippocampus that is important for memory, which is an early site of neurofibrillary tangle pathology in AD (Hyman et al., 1984, 1986; Van Hoesen and Hyman, 1990; Hyman, 1997). Correlations were used to explore relationships between hippocampal subregion and entorhinal volume, which revealed a pattern where the strongest correlations with entorhinal volume were with the hippocampal head, followed by the body and tail. In addition, the hippocampal head was the only subregion to demonstrate a relationship with CSF tau (a reflection of neurofibrillary tangle pathology), which together provide further evidence of pathological disruption of connections between the entorhinal cortex and hippocampal head. These results suggest that atrophy and related cognitive decline is occurring earliest in the hippocampal head, followed by the body and tail, and that the head and body demonstrate the most salient relationships with NP measures of memory, with fewer relationships in the hippocampal tail. This also supports the notion of functional differences along the anterior-posterior axis of this hippocampus.

In addition to regional differences in connectivity, it is possible that anterior-to-posterior differences within the hippocampus are due to cholinergic fiber loss. A higher density of acetyl cholinesterase has been reported in the rostral hippocampus (Rosene and Van Hoesen, 1987). Additionally, when considering the extent to which cholinergic fiber density and loss are evident in hippocampal subfields, a study based on non-human primates reported that there is a higher density in CA3 as compared to dentate gyrus and CA1, though loss of cholinergic innervation in aging is consistent across the longitudinal axis of the hippocampus (Calhoun et al., 2004). CA1 and CA3 have been found to lie primarily within the hippocampal head, and the dentate gyrus primarily within the hippocampal body in humans (Malykhin et al., 2010), which together with the aforementioned data further suggest there is increased cholinergic activity within the head of the hippocampus as compared to the body and tail, and loss of these fibers in AD may contribute to a decline in memory.

With regard to the CSF correlations, because CSF $A\beta_{42}$ has been found to demonstrate a negative correlation with Aß deposition in the brain (Strozyk et al., 2003; Tapiola et al., 2009), the positive correlation between hippocampal volumes and CSF $A\beta_{42}$ is what was expected. These correlations suggest that as hippocampal volume is reduced, CSF measures of $A\beta_{42}$ also become reduced, reflecting increased deposition of Aß in the brain.

Discriminant function analyses revealed that the variables best able to classify by diagnostic group in the large population were AV-Immediate and Delayed, Digit Symbol, and the left hippocampal body volume. When CSF measures were entered into analyses for a subgroup of individuals, $A\beta_{42}$ did come out as a predictor when combined with total hippocampal head or left entorhinal volume (when entorhinal volume was entered), however, accuracy in classification was not improved from that in the overall group with these measures. Interestingly, when all measures were entered, neither CSF nor entorhinal measures came out as predictors, suggesting hippocampal subregions may contribute independent information to group classification.

When assessing MCI stable and converter subjects, only NP measures (Digit Symbol and Categories) were significant predictors of future conversion, and adding CSF measures to a subgroup of MCI participants resulted in a combination of NP, hippocampal head volume, and CSF measures providing a 100% accurate prediction in who would remain stable and who would

decline within a 12 month period. While promising, this was based only on a very small group of participants, and requires additional research on a larger population. In addition, CSF measures of $A\beta_{42}$ were correlated with all hippocampal measures except for the right hippocampal body, supporting that lower CSF $A\beta_{42}$ is related to smaller hippocampal volume.

Overall, the results of this study further support regional differences in function and atrophy in the hippocampus in normal aging, MCI, and AD, and how these subregions relate to other measures including NP tests and CSF levels in the classification of diagnostic group and prediction of future decline. These results additionally suggest the head, body, and tail of the hippocampus may be more useful than total hippocampal volume as biomarkers in the detection of early AD.

Limitations to this study include that only a small subset of the entire ADNI population was included in analyses due to the manual intervention involved in subdividing the hippocampus. Similarly, a limited number of MCI subjects had converted to AD at the 12-month follow-up visit, and even fewer of these subjects had CSF measures available. As MCI subjects are continued to be followed over longer periods of time and a larger number of subjects convert to AD, it is possible that more salient predictors of group classification and prediction of future decline will be evident.

## ACKNOWLEDGEMENTS

Data collection and sharing for this project was funded by the Alzheimer's Disease Neuroimaging Initiative (ADNI). Private sector contributions to ADNI are facilitated by the Foundation for the National Institutes of Health (www.fnih.org, http://www.fnih.org/, http://www.fnih.org, http://www.fnih.org/). The grantee organization is the Northern California Institute for Research and Education, and the study is coordinated by the Alzheimer's Disease Cooperative Study at the University of California, San Diego. ADNI data are disseminated by the Laboratory for Neuro Imaging at the University of California, Los Angeles.

## LITERATURE CITED

Bernasconi N, Bernasconi A, Caramanos Z, Antel SB, Andermann F, Arnold DL. 2003. Mesial temporal damage in temporal lobe epilepsy: A volumetric MRI study of the hippocampus, amygdala and parahippocampal region. Brain 126:462–469.

Blennow K, Wallin A, Agren H, Spenger C, Siegfried J, Vanmechelen E. 1995. Tau protein in cerebrospinal fluid: A biochemical marker for axonal degeneration in Alzheimer disease? Mol Chem Neuropathol 26:231–245.

Bouchard TP, Malykhin N, Martin WR, Hanstock CC, Emery DJ, Fisher NJ, Camicioli RM. 2008. Age and dementia-associated atrophy predominates in the hippocampal head and amygdala in Parkinson's disease. Neurobiol Aging 29:1027–1039.

Bouras C, Hof PR, Giannakopoulos P, Michel JP, Morrison JH. 1994. Regional distribution of neurofibrillary tangles and senile plaques in the cerebral cortex of elderly patients: A quantitative evaluation of a one-year autopsy population from a geriatric hospital. Cereb Cortex 4:138–150.

Bouras C, Hof PR, Morrison JH. 1993. Neurofibrillary tangle densities in the hippocampal formation in a non-demented population define subgroups of patients with differential early pathologic changes. Neurosci Lett 153:131–135.

Bourgeat P, Chetelat G, Villemagne VL, Fripp J, Raniga P, Pike K, Acosta O, Szoeke C, Ourselin S, Ames D, Ellis KA, Martins RN, Masters CL, Rowe CC, Salvado O. 2010. Beta-amyloid burden in the temporal neocortex is related to hippocampal atrophy in elderly subjects without dementia. Neurology 74:121–127.

Braak H, Braak E. 1991. Neuropathological stageing of Alzheimer-related changes. Acta Neuropathol 82:239–259.

Braak H, Braak E, Bohl J. 1993. Staging of Alzheimer-related cortical destruction. Eur Neurol 33:403–408.

Bronen RA, Fulbright RK, Kim JH, Spencer SS, Spencer DD, al-Rodhan NR. 1995. Regional distribution of MR findings in hippocampal sclerosis. AJNR Am J Neuroradiol 16:1193–1200.

Buckner RL, Head D, Parker J, Fotenos AF, Marcus D, Morris JC, Snyder AZ. 2004. A unified approach for morphometric and functional data analysis in young, old, and demented adults using automated atlas-based head size normalization: Reliability and validation against manual measurement of total intracranial volume. Neuroimage 23:724–738.

Buckner RL, Snyder AZ, Shannon BJ, LaRossa G, Sachs R, Fotenos AF, Sheline YI, Klunk WE, Mathis CA, Morris JC, Mintun MA. 2005. Molecular, structural, and functional characterization of Alzheimer's disease: Evidence for a relationship between default activity, amyloid, and memory. J Neurosci 25:7709–7717.

Calhoun ME, Mao Y, Roberts JA, Rapp PR. 2004. Reduction in hippocampal cholinergic innervation is unrelated to recognition memory impairment in aged rhesus monkeys. J Comp Neurol 475:238–246.

Callen DJ, Black SE, Gao F, Caldwell CB, Szalai JP. 2001. Beyond the hippocampus: MRI volumetry confirms widespread limbic atrophy in AD. Neurology 57:1669–1674.

Chen KH, Chuah LY, Sim SK, Chee MW. 2010. Hippocampal region-specific contributions to memory performance in normal elderly. Brain Cogn 72:400–407.

Chetelat G, Landeau B, Eustache F, Mezenge F, Viader F, de la Sayette V, Desgranges B, Baron JC. 2005. Using voxel-based morphometry to map the structural changes associated with rapid conversion in MCI: A longitudinal MRI study. Neuroimage 27: 934–946.

Chetelat G, Villemagne VL, Bourgeat P, Pike KE, Jones G, Ames D, Ellis KA, Szoeke C, Martins RN, O'Keefe GJ, Salvado O, Masters CL, Rowe CC. 2010. Relationship between atrophy and beta-amyloid deposition in Alzheimer disease. Ann Neurol 67:317–324.

Chua EF, Schacter DL, Rand-Giovannetti E, Sperling RA. 2007. Evidence for a specific role of the anterior hippocampal region in successful associative encoding. Hippocampus 17:1071–1080.

Convit A, de Asis J, de Leon MJ, Tarshish CY, De Santi S, Rusinek H. 2000. Atrophy of the medial occipitotemporal, inferior, and middle temporal gyri in non-demented elderly predict decline to Alzheimer's disease. Neurobiol Aging 21:19–26.

Csernansky JG, Wang L, Swank J, Miller JP, Gado M, McKeel D, Miller MI, Morris JC. 2005. Preclinical detection of Alzheimer's disease: Hippocampal shape and volume predict dementia onset in the elderly. Neuroimage 25:783–792.

Dale AM, Fischl B, Sereno MI. 1999. Cortical surface-based analysis. I. Segmentation and surface reconstruction. Neuroimage 9:179–194.

Dale AM, Sereno, MI. 1993. Improved localization of cortical activity by combining EEG and MEG with MRI cortical surface reconstruction: A linear approach. J Cogn Neurosci 5:162–176.

de Leon MJ, Mosconi L, Blennow K, DeSanti S, Zinkowski R, Mehta PD, Pratico D, Tsui W, Saint Louis LA, Sobanska L, Brys M, Li Y, Rich K, Rinne J, Rusinek H. 2007. Imaging and CSF studies in the preclinical diagnosis of Alzheimer's disease. Ann N Y Acad Sci 1097:114–145.

den Heijer T, Geerlings MI, Hoebeek FE, Hofman A, Koudstaal PJ, Breteler MM. 2006. Use of hippocampal and amygdalar volumes on magnetic resonance imaging to predict dementia in cognitively intact elderly people. Arch Gen Psychiatry 63:57–62.

Desikan RS, Fischl B, Cabral HJ, Kemper TL, Guttmann CR, Blacker D, Hyman BT, Albert MS, Killiany RJ. 2008. MRI measures of temporoparietal regions show differential rates of atrophy during prodromal AD. Neurology 71:819–825.

Desikan RS, Segonne F, Fischl B, Quinn BT, Dickerson BC, Blacker D, Buckner RL, Dale AM, Maguire RP, Hyman BT, Albert MS, Killiany RJ. 2006. An automated labeling system for subdividing the human cerebral cortex on MRI scans into gyral based regions of interest. Neuroimage 31:968–980.

Devanand DP, Liu X, Tabert MH, Pradhaban G, Cuasay K, Bell K, de Leon MJ, Doty RL, Stern Y, Pelton GH. 2008. Combining early markers strongly predicts conversion from mild cognitive impairment to Alzheimer's disease. Biol Psychiatry 64:871–879.

Devanand DP, Pradhaban G, Liu X, Khandji A, De Santi S, Segal S, Rusinek H, Pelton GH, Honig LS, Mayeux R, Stern Y, Tabert MH, de Leon MJ. 2007. Hippocampal and entorhinal atrophy in mild cognitive impairment: Prediction of Alzheimer disease. Neurology 68:828–836.

Ekstrom AD, Bazih AJ, Suthana NA, Al-Hakim R, Ogura K, Zeineh M, Burggren AC, Bookheimer SY. 2009. Advances in high-resolution imaging and computational unfolding of the human hippocampus. Neuroimage 47:42–49.

Fischl B, Dale AM. 2000. Measuring the thickness of the human cerebral cortex from magnetic resonance images. Proc Natl Acad Sci USA 97:11050–11055.

Fischl B, Liu A, Dale AM. 2001. Automated manifold surgery: Constructing geometrically accurate and topologically correct models of the human cerebral cortex. IEEE Trans Med Imaging 20: 70–80.

Fischl B, Salat DH, Busa E, Albert M, Dieterich M, Haselgrove C, van der Kouwe A, Killiany R, Kennedy D, Klaveness S, Montillo A, Makris N, Rosen B, Dale AM. 2002. Whole brain segmentation: Automated labeling of neuroanatomical structures in the human brain. Neuron 33:341–355.

Fischl B, Salat DH, van der Kouwe AJ, Makris N, Segonne F, Quinn BT, Dale AM. 2004a. Sequence-independent segmentation of magnetic resonance images. Neuroimage 23(Suppl 1):S69–S84.

Fischl B, Sereno MI, Dale AM. 1999. Cortical surface-based analysis. II. Inflation, flattening, and a surface-based coordinate system. Neuroimage 9:195–207.

Fischl B, van der Kouwe A, Destrieux C, Halgren E, Segonne F, Salat DH, Busa E, Seidman LJ, Goldstein J, Kennedy D, Caviness V, Makris N, Rosen B, Dale AM. 2004b. Automatically parcellating the human cerebral cortex. Cereb Cortex 14:11–22.

Fleisher AS, Sun S, Taylor C, Ward CP, Gamst AC, Petersen RC, Jack CR, Jr, Aisen PS, Thal LJ. 2008. Volumetric MRI vs clinical predictors of Alzheimer disease in mild cognitive impairment. Neurology 70:191–199.

Folstein MF, Folstein SE, McHugh PR. 1975. "Mini-mental state". A practical method for grading the cognitive state of patients for the clinician. J Psychiatr Res 12:189–198.

Fox NC, Warrington EK, Freeborough PA, Hartikainen P, Kennedy AM, Stevens JM, Rossor MN. 1996. Presymptomatic hippocampal atrophy in Alzheimer's disease. A longitudinal MRI study. Brain 119(Pt 6):2001–2007.

Frank RA, Galasko D, Hampel H, Hardy J, de Leon MJ, Mehta PD, Rogers J, Siemers E, Trojanowski JQ. 2003. Biological markers for therapeutic trials in Alzheimer's disease. Proceedings of the biological markers working group; NIA initiative on neuroimaging in Alzheimer's disease. Neurobiol Aging 24:521–536.

Giannakopoulos P, Hof PR, Mottier S, Michel JP, Bouras C. 1994. Neuropathological changes in the cerebral cortex of 1258 cases from a geriatric hospital: Retrospective clinicopathological evaluation of a 10-year autopsy population. Acta Neuropathol 87:456–468.

Hackert VH, den Heijer T, Oudkerk M, Koudstaal PJ, Hofman A, Breteler MM. 2002. Hippocampal head size associated with verbal memory performance in nondemented elderly. Neuroimage 17:1365–1372.

Han X, Jovicich J, Salat D, van der Kouwe A, Quinn B, Czanner S, Busa E, Pacheco J, Albert M, Killiany R, Maguire P, Rosas D, Makris N, Dale A, Dickerson B, Fischl B. 2006. Reliability of MRI-derived measurements of human cerebral cortical thickness: The effects of field strength, scanner upgrade and manufacturer. Neuroimage 32:180–194.

Haroutunian V, Purohit DP, Perl DP, Marin D, Khan K, Lantz M, Davis KL, Mohs RC. 1999. Neurofibrillary tangles in nondemented elderly subjects and mild Alzheimer disease. Arch Neurol 56:713–718.

Hyman BT. 1997. The neuropathological diagnosis of Alzheimer's disease: Clinical–pathological studies. Neurobiol Aging 18:S27–S32.

Hyman BT, Van Hoesen GW, Damasio AR, Barnes CL. 1984. Alzheimer's disease: Cell-specific pathology isolates the hippocampal formation. Science 225:1168–1170.

Hyman BT, Van Hoesen GW, Kromer LJ, Damasio AR. 1986. Perforant pathway changes and the memory impairment of Alzheimer's disease. Ann Neurol 20:472–481.

Jack CR, Jr, Bernstein MA, Fox NC, Thompson P, Alexander G, Harvey D, Borowski B, Britson PJ, Whitwell LJ, Ward C, Dale AM, Felmlee JP, Gunter JL, Hill DL, Killiany R, Schuff N, Fox-Bosetti S, Lin C, Studholme C, DeCarli CS, Krueger G, Ward HA, Metzger GJ, Scott KT, Mallozzi R, Blezek D, Levy J, Debbins JP, Fleisher AS, Albert M, Green R, Bartzokis G, Glover G, Mugler J, Weiner MW. 2008a. The Alzheimer's Disease Neuroimaging Initiative (ADNI): MRI methods. J Magn Reson Imaging 27:685–691.

Jack CR, Jr, Lowe VJ, Senjem ML, Weigand SD, Kemp BJ, Shiung MM, Knopman DS, Boeve BF, Klunk WE, Mathis CA, Petersen RC. 2008b. 11C PiB and structural MRI provide complementary information in imaging of Alzheimer's disease and amnestic mild cognitive impairment. Brain 131:665–680.

Jack CR, Jr, Shiung MM, Weigand SD, O'Brien PC, Gunter JL, Boeve BF, Knopman DS, Smith GE, Ivnik RJ, Tangalos EG, Petersen RC. 2005. Brain atrophy rates predict subsequent clinical conversion in normal elderly and amnestic MCI. Neurology 65:1227–1231.

Jovicich J, Czanner S, Greve D, Haley E, van der Kouwe A, Gollub R, Kennedy D, Schmitt F, Brown G, Macfall J, Fischl B, Dale A. 2006. Reliability in multi-site structural MRI studies: Effects of gradient non-linearity correction on phantom and human data. Neuroimage 30:436–443.

Kaplan EF, Goodglass H, Weintraub S. 1983. The boston naming test. Philadelphia: Lea and Febiger.

Killiany RJ, Hyman BT, Gomez-Isla T, Moss MB, Kikinis R, Jolesz F, Tanzi R, Jones K, Albert MS. 2002. MRI measures of entorhinal cortex vs hippocampus in preclinical AD. Neurology 58:1188–1196.

Lepage M, Habib R, Tulving E. 1998. Hippocampal PET activations of memory encoding and retrieval: The HIPER model. Hippocampus 8:313–322.

Malykhin NV, Lebel RM, Coupland NJ, Wilman AH, Carter R. 2010. In vivo quantification of hippocampal subfields using 4.7 T fast spin echo imaging. Neuroimage 49:1224–1230.

Martin SB, Smith CD, Collins HR, Schmitt FA, Gold BT. 2010. Evidence that volume of anterior medial temporal lobe is reduced in seniors destined for mild cognitive impairment. Neurobiol Aging 31:1099–1106.

Mormino EC, Kluth JT, Madison CM, Rabinovici GD, Baker SL, Miller BL, Koeppe RA, Mathis CA, Weiner MW, Jagust WJ. 2009. Episodic memory loss is related to hippocampal-mediated beta-amyloid deposition in elderly subjects. Brain 132:1310–1323.

Mueller SG, Stables L, Du AT, Schuff N, Truran D, Cashdollar N, Weiner MW. 2007. Measurement of hippocampal subfields and age-related changes with high resolution MRI at 4T. Neurobiol Aging 28:719–726.

Ouchi Y, Nobezawa S, Okada H, Yoshikawa E, Futatsubashi M, Kaneko M. 1998. Altered glucose metabolism in the hippocampal head in memory impairment. Neurology 51:136–142.

Price JL, Davis PB, Morris JC, White DL. 1991. The distribution of tangles, plaques and related immunohistochemical markers in healthy aging and Alzheimer's disease. Neurobiol Aging 12:295–312.

Price JL, Morris JC. 1999. Tangles and plaques in nondemented aging and "preclinical" Alzheimer's disease. Ann Neurol 45:358–368.

Reckess G. Antecedent biomarkers in Alzheimer's disease: Uses, limitations, and future directions for research. In: Morris JC, Chair, editor. 2003. St. Louis, Missouri: Washington University Alzheimer's Disease Research Center. http://www.alzforum.org/res/enab/workshops/biomarkers.asp.

Reitan RM. 1958. Validity of the trail making tests as an indicator of organic brain damage. Perception Motor Skills 8:253–266.

Rey A. 1964. L'Examen clinique en psychologie. Paris: Presses Universitaires de France.

Risacher SL, Saykin AJ, West JD, Shen L, Firpi HA, McDonald BC. 2009. Baseline MRI predictors of conversion from MCI to probable AD in the ADNI cohort. Curr Alzheimer Res 6:347–361.

Rosazza C, Minati L, Ghielmetti F, Maccagnano E, Erbetta A, Villani F, Epifani F, Spreafico R, Bruzzone MG. 2009. Engagement of the medial temporal lobe in verbal and nonverbal memory: Assessment with functional MR imaging in healthy subjects. AJNR Am J Neuroradiol 30:1134–1141.

Rosen WG, Mohs RC, Davis KL. 1984. A new rating scale for Alzheimer's disease. Am J Psychiatry 141:1356–1364.

Rosene DL, Van Hoesen GV. 1987. The hippocampal formation of the primate brain: A review of some comparative aspects of cytoarchitecture and connections. In: Jones EG, Peters A, editors. Cerebral Cortex. New York: Plenum Press. p 345–456.

Segonne F, Dale AM, Busa E, Glessner M, Salat D, Hahn HK, Fischl B. 2004. A hybrid approach to the skull stripping problem in MRI. Neuroimage 22:1060–1075.

Segonne F, Pacheco J, Fischl B. 2007. Geometrically accurate topology-correction of cortical surfaces using nonseparating loops. IEEE Trans Med Imaging 26:518–529.

Shaw LM, Vanderstichele H, Knapik-Czajka M, Clark CM, Aisen PS, Petersen RC, Blennow K, Soares H, Simon A, Lewczuk P, Dean R, Siemers E, Potter W, Lee VM, Trojanowski JQ. 2009. Cerebrospinal fluid biomarker signature in Alzheimer's disease neuroimaging initiative subjects. Ann Neurol 65:403–413.

Storandt M, Mintun MA, Head D, Morris JC. 2009. Cognitive decline and brain volume loss as signatures of cerebral amyloid-beta peptide deposition identified with Pittsburgh compound B: Cognitive decline associated with Abeta deposition. Arch Neurol 66:1476–1481.

Strange BA, Fletcher PC, Henson RN, Friston KJ, Dolan RJ. 1999. Segregating the functions of human hippocampus. Proc Natl Acad Sci USA 96:4034–4039.

Strozyk D, Blennow K, White LR, Launer LJ. 2003. CSF Abeta 42 levels correlate with amyloid-neuropathology in a population-based autopsy study. Neurology 60:652–656.

Tapiola T, Alafuzoff I, Herukka SK, Parkkinen L, Hartikainen P, Soininen H, Pirttila T. 2009. Cerebrospinal fluid {beta}-amyloid 42 and tau proteins as biomarkers of Alzheimer-type pathologic changes in the brain. Arch Neurol 66:382–389.

Tapiola T, Overmyer M, Lehtovirta M, Helisalmi S, Ramberg J, Alafuzoff I, Riekkinen P, Sr, Soininen H. 1997. The level of cerebrospinal fluid tau correlates with neurofibrillary tangles in Alzheimer's disease. Neuroreport 8:3961–3963.

Theysohn JM, Kraff O, Maderwald S, Schlamann MU, de Greiff A, Forsting M, Ladd SC, Ladd ME, Gizewski ER. 2009. The human hippocampus at 7 T—In vivo MRI. Hippocampus 19:1–7.

Ulrich J. 1985. Alzheimer changes in nondemented patients younger than sixty-five: Possible early stages of Alzheimer's disease and senile dementia of Alzheimer type. Ann Neurol 17:273–277.

Van Hoesen GW, Hyman BT. 1990. Hippocampal formation: Anatomy and the patterns of pathology in Alzheimer's disease. Prog Brain Res 83:445–457.

Van Leemput K, Bakkour A, Benner T, Wiggins G, Wald LL, Augustinack J, Dickerson BC, Golland P, Fischl B. 2009. Automated segmentation of hippocampal subfields from ultra-high resolution in vivo MRI. Hippocampus 19:549–557.

Walhovd KB, Fjell AM, Brewer J, McEvoy LK, Fennema-Notestine C, Hagler DJ, Jr, Jennings RG, Karow D, Dale AM. 2010. Combining MR imaging, positron-emission tomography, and CSF biomarkers in the diagnosis and prognosis of Alzheimer disease. AJNR Am J Neuroradiol 31:347–354.

Witthaus H, Mendes U, Brune M, Ozgurdal S, Bohner G, Gudlowski Y, Kalus P, Andreasen N, Heinz A, Klingebiel R, Juckel G. 2010. Hippocampal subdivision and amygdalar volumes in patients in an at-risk mental state for schizophrenia. J Psychiatry Neurosci 35:33–40.

Yushkevich PA, Avants BB, Das SR, Pluta J, Altinay M, Craige C. 2010. Bias in estimation of hippocampal atrophy using deformation-based morphometry arises from asymmetric global normalization: An illustration in ADNI 3 T MRI data. Neuroimage 50:434–445.

Yushkevich PA, Avants BB, Pluta J, Das S, Minkoff D, Mechanic-Hamilton D, Glynn S, Pickup S, Liu W, Gee JC, Grossman M, Detre JA. 2009. A high-resolution computational atlas of the human hippocampus from postmortem magnetic resonance imaging at 9.4 T. Neuroimage 44:385–398.

Zeineh MM, Engel SA, Bookheimer SY. 2000. Application of cortical unfolding techniques to functional MRI of the human hippocampal region. Neuroimage 11:668–683.

Zeineh MM, Engel SA, Thompson PM, Bookheimer SY. 2001. Unfolding the human hippocampus with high resolution structural and functional MRI. Anat Rec 265:111–120.